

1 **Evaluating pesticide degradation in artificial wetlands with compound-specific**
2 **isotope analysis: a case study with the fungicide dimethomorph**

3

4

5

6 *Tetyana Gilevska¹, Sylvain Payraudeau¹, Gwenaël Imfeld¹*

7

8 ¹ Université de Strasbourg, CNRS/ENGEES, ITES UMR 7063, Institut Terre et Environnement de
9 Strasbourg, Strasbourg, France

10

11

12

13

14

15

16

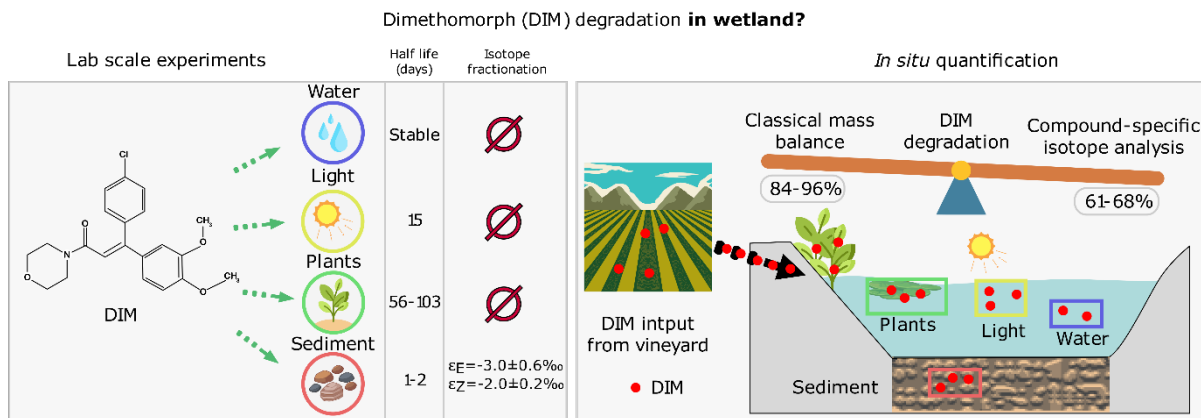
17

18

19

20

21 Manuscript for Science of the Total Environment



22

23 **Keywords:** compound-specific isotope analysis; pesticides; wetland; isomer; biodegradation

24 **Abstract**

25 Pesticide degradation in wetland systems intercepting agricultural runoff is often

26 overlooked and mixed with other dissipation processes when estimated based on pesticide

27 concentrations alone. This study focused on the potential of compound-specific isotope analysis

28 (CSIA) to estimate pesticide degradation in a stormwater wetland receiving pesticide runoff from

29 a vineyard catchment. The fungicide dimethomorph (DIM), with diastereoisomers E and Z, was

30 the prevalent pesticide in the runoff entering the wetland from June to September 2020. DIM Z,

31 the most commonly detected isomer, exhibited a significant change ($\Delta^{13}\text{C} > 3\text{‰}$) in its carbon

32 isotopic composition in the wetland water compared to the runoff and commercial formulation,

33 indicating degradation. Laboratory DIM degradation assays, including photodegradation and

34 biodegradation in oxic wetland water with and without aquatic plants and in anoxic sediments,

35 indicated that DIM degradation mainly occurred in the wetland sediments. The rapid degradation

36 (E: $t_{1/2} = 1.2 \pm 0.6$, Z: $t_{1/2} = 1.5 \pm 0.8$ days) of DIM in the wetland sediment led to significant carbon

37 isotopic fractionation ($\epsilon_{\text{DIM-E}} = -3.0 \pm 0.6\text{‰}$, $\epsilon_{\text{DIM-Z}} = -2.0 \pm 0.2\text{‰}$). In contrast, no significant

38 isotope fractionation occurred during DIM photodegradation, despite the rapid isomerization of the

39 E isomer to the Z isomer and a half-life of 15.3 ± 2.2 days for both isomers. DIM degradation was
40 slow (E: $t_{1/2} = 56-62$ days, Z: $t_{1/2} = 82-103$ days) in oxic water with plants, while DIM persisted
41 (120 days) in water without plants. DIM CSIA was thus used to evaluate the *in situ* biodegradation
42 of DIM Z in the wetland. The DIM Z degradation estimates based on a classical concentration mass
43 balance (86-94%) were slightly higher than those from the isotopic mass balance (61-68%). This
44 study highlights the potential of CSIA to conservatively evaluate pesticide degradation in wetland
45 systems, offering a reliable alternative to classical labor-intensive mass balance approaches.

46

47 **1. Introduction**

48 Pesticide runoff from agricultural catchments poses serious environmental risks to
49 downstream ecosystems (Tang et al., 2021). Nonetheless, pesticide use may increase in the coming
50 decades as a result of climate change, pest prevalence, introduction of invasive species, and
51 pesticide resistance (Koli et al., 2019). Although the reduction or elimination of pesticide use
52 remains the best option to limit impacts on human and ecosystem health, ponds and constructed
53 wetlands at catchment outlets can partially intercept surface runoff events and protect surface
54 waters from pesticide pollution (Maillard et al., 2011). In fact, artificial wetlands offer a variety of
55 biogeochemical conditions across wetland compartments (i.e., water, sediments, plants, suspended
56 solids), driving the dissipation of organic pollutants from agricultural catchments (Imfeld et al.,
57 2021). Pesticide dissipation, i.e., the apparent decrease in pesticide concentrations in wetlands, is
58 the result of several dissipation processes, including sorption to sediments, plant uptake, and biotic
59 and abiotic degradation. Only pesticide degradation can lead to the complete mineralization of
60 pesticides, although intermediate and potentially toxic transformation products (TPs) may be

61 formed. However, the contribution of pesticide degradation to the overall dissipation in stormwater
62 wetlands receiving pesticide runoff from agricultural catchments remains mostly unknown since
63 dissipation processes co-occur and may vary over time.

64 The efficiency of wetland systems in removing pesticides is generally estimated based on a
65 work-intensive, often uncertain, and costly mass balance comparing inlet and outlet fluxes of
66 pesticides. A major drawback of this black-box approach is that processes contributing to overall
67 pesticide dissipation, including degradation and sorption, remain elusive (Grégoire et al., 2009)
68 and depend on the physicochemical properties of the pesticide. Therefore, the underlying
69 hypothesis of this study is that better quantification of processes contributing to pesticide
70 dissipation in wetland compartments can facilitate the evaluation of the potential of wetland
71 systems to degrade pesticides and to form transformation products (TPs).

72 In contrast to mass balance approaches based on concentration analysis, compound-specific
73 isotope analysis (CSIA) may help differentiate degradative (i.e., involving molecular bond
74 cleavage) or nondegradative processes leading to a decrease in the concentration of a specific
75 contaminant molecule. CSIA is used to measure the ratio of a heavy isotope of an element (^HE) to
76 the light stable isotope (^LE) in an individual compound (Urey, 1947). During reactions, chemical
77 bonds containing exclusively light isotopes (e.g., ^{12}C) are cleaved at slightly faster rates than those
78 containing heavier isotopes (e.g., ^{13}C). This may lead to a change in the isotope ratio in the
79 remaining, nondegraded contaminant fraction. Combined with concentration analysis, pesticide
80 CSIA can provide multiple lines of evidence for pesticide transformation in wetlands and allow for
81 the quantification of the extent of degradation when corresponding isotope fractionation values (ϵ)
82 are known. Only a few studies have investigated pesticide degradation in surface water using CSIA

83 (Alvarez-Zaldivar et al., 2018; Gilevska et al., 2022a; Masbou et al., 2022; Schreglmann et al.,
84 2013; Suchana et al., 2022), and reference studies on pesticide CSIA in wetland systems are
85 currently limited (Chen et al., 2022) .

86 In this context, the purpose of this study is to determine the contribution of pesticide
87 degradation to overall pesticide dissipation in a stormwater wetland collecting pesticide runoff
88 from a vineyard catchment. In previous studies, a mass balance approach based on concentration
89 data enabled the quantification of pesticide partitioning, distribution, and dissipation in the
90 compartments of a stormwater wetland (Grégoire et al., 2010; Maillard et al., 2011). Although
91 these studies underscored that the stormwater wetland acted as a pesticide sink, with dissipation
92 depending on pesticide properties and involved compartments, direct proof and reliable estimates
93 of pesticide degradation are currently missing. Dimethomorph (DIM), a morpholine fungicide,
94 prevailed in pesticide runoff entering the wetland and in the wetland over the studied period. DIM
95 was thus used as a model compound to examine pesticide degradation using CSIA. DIM is a
96 racemic compound, i.e., composed of equal proportions of the diastereoisomers E and Z, with
97 isomer Z exhibiting fungicidal activity by inhibiting ergosterol synthesis (Avetta et al., 2014).
98 Laboratory experiments were set up to retrieve reference isotope and isomer (IF(Z)) fractionation
99 values for photodegradation and biodegradation in wetland compartments (i.e., water, sediments,
100 and plants), allowing for the quantification of degradation of DIM Z, the most commonly detected
101 isomer, using CSIA. A comparison of the mass balances based on field DIM Z concentration and
102 stable isotope data to evaluate pesticide degradation in the stormwater wetland underscored the
103 potential of pesticide CSIA to improve the evaluation of the natural attenuation of pesticides in
104 wetland systems.

105

106 2. Material and Methods

107 2.1. Study wetland

108 The stormwater wetland (47°57'9 N, 07°17'3 E) was located at the outlet of a 42.7 ha
109 vineyard catchment area in Alsace (eastern France). In 2020, conventional vineyards, with
110 applications of synthetic pesticides, covered 50% (14.5 ha) of the vineyard area of the catchment,
111 involving more than 30 wine growers. The characteristics of the vineyard catchment and the
112 stormwater wetland have been detailed previously (Duplay et al., 2014; Grégoire et al., 2010;
113 Imfeld et al., 2020; Maillard et al., 2011). Six fungicides (DIM Z and E, cyprodinil, metalaxyl,
114 pyrimethanil, tebuconazole, tetraconazole) and four herbicides (pendimethalin, *S*-metolachlor,
115 atrazine, terbuthylazine) were selected in this study based on the aforementioned studies and their
116 compatibility for CSIA. Volatility was a key criterion for applying CSIA, ensuring that the
117 compounds could be analyzed by gas chromatography with high precision and accuracy for CSIA.
118 Briefly, the study wetland (319 m²) consisted of a forebay (215 m²) and a 0.6 m deep gravel filter
119 containing a maximum volume of 62 m³ to increase the hydraulic retention time and dissipation
120 efficiency (Figure S1) (Maillard and Imfeld, 2014). The wetland has a maximum storage capacity
121 of 1108 m³. Six piezometers of 0.6m depth were located in the gravel filter. The sediment was
122 partly (75%) excavated from the forebay area in February 2020 to increase the water storage
123 capacity and reduce flood risk. As a result, water stagnated in the forebay, with water depths
124 ranging from 0.25 m to 0.40 m from June to September 2020, corresponding to a dead water volume
125 of 63 m³ upstream of the outflow pipes. The vegetation, i.e., *Phragmites australis* (common reed),
126 *Lemna minor* (common duckweed), *Typha Latifolia* (common cattail), coverage increased from
127 approximately 50% of the forebay in April up to 100% from the end of July until September 2020.

128

129 2.2. Sampling

130 *Water.* From June 2nd to September 28th, water samples (300 mL) were collected at the
131 wetland inlet every 3 m³ using an automatic flow proportional sampler (6712FR ISCO Teledyne
132 automatic sampler with a maximum capacity of 24 L, Lincoln, NE, USA). In parallel, four grab
133 water subsamples (2.5 L) were collected weekly with a beaker using a telescopic pole from four
134 representative spots in the wetland forebay. The subsamples were then pooled into a weekly
135 composite sample. Water was additionally sampled monthly from the piezometers in the gravel
136 filter (2 L per piezometer, a total of 12 L) after a 2-minute purge.

137 Water samples were successively filtered at 11 µm through grade one cellulose (Whatman
138 1001-047) and 0.45 µm cellulose acetate membrane filters and stored at 4 °C until further analysis.
139 The hydrochemical composition (Supplementary material (SI), Table S1) of water samples was
140 determined by ion chromatography (IC) and inductively coupled plasma atomic emission
141 spectroscopy (ICP–AES) using standard analytical procedures (NF/ISO) (Lucas et al., 2010).
142 Conductivity, temperature, and pH were directly measured in the wetland water using WTW multi
143 350i sensors (WTW, Weilheim, Germany). Total suspended solids (TSS) were obtained from the
144 inlet, forebay, and piezometer water samples by passing the water through 0.45 µm filters and
145 weighing the mass of the suspended solids after drying.

146 *Polar Organic Chemical Integrative Samplers (POCIS).* POCIS were used to obtain
147 integrative isotope signatures of pesticides in the forebay area over time in water samples and to
148 compare the integrative signatures with punctual isotope signatures from grab samples. POCIS
149 were deployed in triplicate in the stormwater wetland forebay area over three consecutive periods
150 of 28 days, from June 30th to September 22nd. The POCIS were transported on ice to the laboratory
151 and extracted within 15 h after collection or frozen at –20 °C before extraction (Gilevska et al.,
152 2022a). Briefly, each POCIS was opened to transfer the sorbent to an SPE cartridge, which was

153 then covered by HDPE frits. The samples were eluted using the SPE procedure, with cartridges
154 dried for 20 minutes with N₂ nitrogen and eluted with successive 3 mL volumes of MeOH and
155 MeOH:EtOAc (Lissalde et al., 2011). The extracts were evaporated and reconstituted in ACN.

156 *Sediment.* The top (0-10 cm) forebay sediments were sampled with a stainless-steel shovel
157 that was cleaned with ultrapure water and ethanol and wiped between collections. Sediment
158 samples were sieved through a 2-mm mesh and stored at 4 °C before analysis in tightly closed glass
159 bottles. The physicochemical characteristics of the sieved sediment samples (Table S2) were
160 measured using standard analytical procedures (NF/ISO) (Lucas et al., 2010).

161 *Vegetation.* Common reeds, common duckweed, and common cattail individuals ($n_{\text{total}}=20$)
162 were sampled monthly from June to September from the wetland forebay and separated into roots
163 and aerial parts (except for duckweed). Plant roots and aerial parts were washed by shaking the
164 roots for 10 min in ultrapure water. The water was replaced several times until the sediment was
165 entirely separated from the roots (Barillot et al., 2013). A 0.9% NaCl solution was then used twice
166 to rinse the plant material to remove rhizosphere sediments. The plant material was homogenized
167 with a hand blender (Bosch MSM66110) and frozen at -20 °C until further use.

168 **2.3. Pesticide extraction**

169 The pesticide extraction method for water samples (inlet runoff, forebay, piezometer and
170 from DIM degradation assays) was adapted from USA EPA method 525.2, and extraction was
171 carried out using an AutoTrace 280 solid-phase extraction (SPE) system (Dionex®, CA, USA)
172 (Elsayed et al., 2014). The pesticides obtained from the sediment, soil, or plants were extracted
173 using a solid-liquid extraction protocol (modified ultrasonic-assisted extraction) described

174 previously (Gilevska et al., 2022b). The POCIS were handled and extracted separately using SPE
175 (Gilevska et al., 2022a).

176 **2.4. DIM degradation assays**

177 Since DIM prevailed in pesticide runoff entering the wetland and in the wetland over the
178 studied period (60% of the total mass of the ten targeted pesticides), DIM was used as a model
179 compound to examine pesticide degradation in the wetland. Pseudo first-order kinetics were
180 assumed in all degradation experiments (SI, Section S2).

181 **2.4.1. DIM photodegradation**

182 DIM direct and indirect (i.e., with nitrate and dissolved organic carbon) photodegradation
183 in an aqueous solution was performed under constant simulated sunlight (Q-Sun Xe 1 chamber)
184 with 0.68 W/m^2 at 340 nm. The direct photodegradation of DIM takes place through direct
185 interaction with light, while indirect photodegradation typically involves reactive intermediates or
186 products formed during a photochemical reaction during DIM degradation. The light intensity
187 corresponded to the Solar Maximum condition, i.e., global noon sunlight at normal incidence on
188 the summer solstice. The irradiance time was later normalized according to 5.21 peak sun hours
189 per day in June in France (Honsberg and Bowden, 2019). The aqueous solution was prepared to
190 mimic the wetland hydrochemical conditions (Table S1) with nitrate (2 mg/L sodium nitrate salts),
191 10 mM phosphate buffer ($\text{Na}_2\text{HPO}_4 \cdot 7\text{H}_2\text{O}$ 1.084 g/ NaH_2PO_4 408 mg), Suwanee River fulvic acid
192 (20 mg/L - carbon content ~53%) and DIM (0.5 mg/L). Duplicate samples were extracted on Days
193 1, 2, 3, 4, 5, 7, and 8. Controls were kept in the dark at 60 °C (mimicking Q-Sun Xe 1 chamber
194 temperature) and were extracted on Days 1, 4, 6, and 8. In parallel, an experiment with 0.5 mg/L
195 DIM in distilled water was set up to account for direct photolysis (i.e., DIM transformation as a

196 consequence of DIM light absorption), and samples were extracted on Days 1, 4, and 8.
197 Considering the low (0.001 mPa) vapour pressure of DIM, no significant DIM volatilization was
198 expected, and any volatilization was accounted for in the dark control experiment. Degradation
199 kinetics were expressed as the sum of Z and E isomers due to the possible isomerization of E into
200 Z upon irradiation (Avetta et al., 2014).

201 **2.4.2. DIM degradation in wetland water**

202 DIM dissipation was investigated in well-homogenized, oxic wetland water microcosms
203 consisting of 60 mL vials filled with 40 mL of water spiked with DIM (0.5 mg/L) and crimped
204 with PTFE caps (Interchim®). A Rotilabo® PTFE syringe filter (0.2 µm) mounted on a syringe tip
205 was used to maintain oxic conditions while avoiding contamination (Torabi et al., 2020). Duplicate
206 microcosms were incubated in the dark at room temperature (20 ± 1 °C) and maintained under
207 constant shaking (orbital shaker, 80 rpm). Duplicate controls were prepared with autoclaved
208 wetland water following the same procedure as above. Four blanks were prepared with DI water
209 without DIM to account for the background matrix of the wetland water samples. Samples were
210 collected on Days 1, 5, 10, 15, 30, and 120. The controls were sampled on Days 1, 30, and 120,
211 and the blanks were sampled on Days 1 and 120.

212 **2.4.3. DIM degradation in wetland water with common duckweed**

213 Common duckweed collected from the stormwater wetland was used to examine DIM
214 degradation in the presence of plants. Our experiment focused on the combined effect of DIM
215 degradation within the plant and by the root microbiome while accounting for DIM uptake by the
216 plants by following temporal changes of DIM concentrations within the plant. A total of 50
217 microcosms were set up in 40 mL beakers, including six treatments. The effect of common

218 duckweed on DIM degradation was examined in microcosms with autoclaved and nonautoclaved
219 wetland water. In parallel, DIM degradation in the absence of plants but with reduced natural light
220 exposure to mimic plant coverage in the wetland was examined in dark (D) and semidark (SD)
221 microcosms. The semidark and dark light control microcosms were wrapped in aluminium foil
222 from the top, with the semidark having five holes (\O : 2 mm) on the top cap. In parallel, six blanks
223 with DI water (processional blank, PB) and four microcosms with nonspiked wetland water and
224 plant material (background blank, BB) were set up. All beakers were wrapped with pierced
225 transparent foil to limit evaporation and covered with aluminium foil up to the water level. The
226 microcosms with common duckweed and autoclaved and nonautoclaved wetland water were
227 sampled on Days 1, 7, 15, 20, 27, 37, and 45. The control (D and SD) and blank (PB, BB) samples
228 were collected on Days 1, 15, 27, and 45.

229 **2.4.4. DIM degradation in wetland sediment**

230 DIM degradation was evaluated in anoxic (Maillard and Imfeld, 2014) (Table S1) wetland
231 sediment. The sieved sediment was spiked with an aqueous DIM solution (20 $\mu\text{g/g}$, racemic
232 mixture of Z and E isomers), thoroughly homogenized, and 20 g (wet weight) of sediment was
233 distributed into twenty-one 40 mL glass vials. The procedure was repeated using autoclaved
234 (autoclaved three cycles, 120°C, 20 min) sediment as an abiotic control. Six additional background
235 controls that consisted of 20 g of sediment were spiked with DI water only without DIM. The vials
236 were capped with blue butyl rubber stoppers and incubated under a N_2 atmosphere. Nonsterile and
237 sterile (autoclaved) triplicate vials were collected on Days 0, 5, 6, 7, 8, and 10 and extracted as
238 described above.

239 **2.5. Chemical analysis**

240 **2.5.1. Pesticide quantification and isomer analysis**

241 DIM and other pesticides were quantified with a gas chromatograph (GC, Trace 1300, 172
242 Thermo Fisher Scientific) coupled to a mass spectrometer (MS, ISQ™, Thermo Fisher 173
243 Scientific) (Masbou et al., 2018). Chromatographic separation was performed with a TG–5MS
244 column (30 m × 0.25 mm ID, 0.25 μm film thicknesses). The mass spectrometry and GC parameters
245 are provided in SI, Section S3.

246 Changes in the E/Z ratios of DIM were calculated with the isomer fractionation $IF(Z)$
247 (Equation S3) (Masbou et al., 2022), with $IF(Z) = 0.5$ and $IF(Z) > 0.5$ featuring a racemic mixture
248 and enrichment in DIM Z, respectively.

249 **2.5.2. DIM CSIA**

250 The concentrations of DIM Z in the wetland water throughout the sampling campaign ($\bar{X} \pm$
251 σ : 306 ± 534 ng/L) were sufficient for carbon CSIA, whereas DIM E concentrations ($\bar{X} \pm \sigma$: $93 \pm$
252 148 ng/L) were insufficient. The carbon stable isotope values ($\delta^{13}C$) of DIM Z were measured
253 using a GC-C-IRMS system consisting of a TRACE™ Ultra gas chromatograph (ThermoFisher
254 Scientific) coupled via a GC IsoLink/Conflow IV interface to an isotope ratio mass spectrometer
255 (DeltaVplus, ThermoFisher Scientific) (Masbou et al., 2022). To ensure measurement accuracy,
256 standard injections with known isotopic compositions of DIM (Z and E isomers), characterized by
257 elemental analyzer IRMS, were performed every six samples. The reproducibility of $\delta^{13}C$
258 measurements was ± 0.4 ‰ ($n \geq 3$). The total uncertainty in carbon isotopic measurements,
259 including precision, accuracy, and reproducibility, was ± 0.6 ‰ ($n = \geq 3$). All isotopic measurements
260 are reported in delta notation (Coplen, 2011) relative to an international isotopic scale (Vienna Pee
261 Dee Belemnite).

262 Isotope fractionation values (ϵ_E), that relate a change in δ^{HE} to the extent of degradation,
263 were derived from the Rayleigh equation without forcing the regression line through the origin
264 (Scott et al., 2004):

$$\ln\left(\frac{\delta^{HE}(t) + 1}{\delta^{HE}_0 + 1}\right) = \epsilon_E \times \ln\left(\frac{c(t)}{c_0}\right) \quad \text{Equation 1}$$

265 where δ^{HE}_0 and $\delta^{HE}(t)$ represent the isotope signatures at time 0 and t of degradation, respectively,
266 whereas $c(t)/c_0$ is the fraction of remaining pesticide at time t.

267 The extent of biodegradation B, expressed in % (Hunkeler et al., 2008) was calculated using
268 the ϵ_E value determined in this study, according to Equation 2. A large (>60%) biodegradation
269 extent is typically required to observe significant ($\Delta^{13C} > 2 \text{ ‰}$) carbon isotope fractionation in
270 large molecules like DIM, as the magnitude of fractionation decreases with increasing carbon
271 number.

$$B = \left(1 - \left(\frac{\delta^{HE}(t) + 1}{\delta^{HE}_0 + 1}\right)^{\frac{1}{\epsilon_E}}\right) \times 100 \quad \text{Equation 2}$$

272

273 **2.6. Mass balance calculations**

274 **2.6.1. Hydrological mass balance**

275 A simple hydrological model of the wetland provided the filling-emptying dynamics and
276 the water volumes of the forebay and gravel compartments of the wetland during the study period

277 (SI, Section S4). The model included water discharge at the wetland inlet from the upstream
278 catchment, direct rainfall, evapotranspiration, and outflow.

279 **2.6.2. Pesticide mass balance from concentration data**

280 The pesticide mass stored in the wetland (M_x) on a weekly basis or over different periods,
281 depending on the hydrological functioning of the wetland, was calculated with Equation 3:

$$282 \quad M_x = \sum^4 M_{dissolved} + M_{TSS} + M_{plant} + M_{sediment} \quad \text{Equation 3}$$

283 where four pools of pesticide mass (mg) are considered: the dissolved phase ($M_{dissolved}$) and a total
284 suspended solid (M_{TSS}) in water stored in the wetland, the uptaken mass in plants (M_{plant}), and the
285 sorbed mass in wetland sediments ($M_{sediment}$) (Table S3).

286 The weekly mass load of pesticides at the wetland inlet, considering the pesticide mass in
287 both the dissolved and the suspended solid phases in inlet samples, was calculated with Equation
288 4:

$$289 \quad M_{inlet,x} = M_{dissolved_inlet} + M_{TSS_inlet} \quad \text{Equation 4}$$

290 The extent of pesticide degradation during periods without outflowing water was calculated
291 with Equation 5:

$$292 \quad \text{Degradation (\%)} = \frac{M_x}{M_{x-1} + \sum M_{inlet,x}} \times 100 \quad \text{Equation 5}$$

293 where (M_x) is the pesticide mass stored in the current week, (M_{x-1}) is the pesticide mass stored in
294 the previous week or beginning of the period, and ($\sum M_{inlet,x}$) is the sum of all the mass loads from
295 the inlet during the evaluated period.

296 Assumptions for the mass balance, including plant density, weight and coverage, and
297 sediment depth, are provided in Table S3.

298 **2.6.3. Isotope mass balance**

299 The isotope mass balance was calculated on a weekly basis or for a defined period, i.e. wet
 300 or dry periods when entering runoff or stored volume did or did not generate outflow, respectively.
 301 To estimate DIM Z degradation in the wetland, two different calculations were used, depending on
 302 the presence or absence of DIM Z runoff at the inlet. Equation 2 was used to quantify DIM Z
 303 degradation in a period without an incoming runoff. Here, $\delta^{13}C_x$ measured at week x in the forebay
 304 was used as ($^HE_{(t)}$), while $\delta^{13}C_{x-1}$ measured at the beginning of the period was used as (δ^HE_0).

305 When runoff entered the wetland, the extent of DIM Z degradation was calculated using
 306 Equation 2 with the ($\delta^{13}C_x$) value of DIM Z measured in week x in the forebay as ($^HE_{(t)}$) and (δ^HE_0)
 307 calculated with Equation 6:

$$308 \quad \delta^HE_{(0)} = \frac{(M_{x-1} \times \delta^{13}C_{x-1} + M_{x,inlet} \times \delta^{13}C_{x,inlet})}{(M_{x-1} + M_{inlet,x})} \quad \text{Equation 6}$$

309 where (M_{x-1}) is the mass stored in the forebay the week before, ($M_{x,inlet}$) is the DIM Z load at the
 310 inlet in week x, and ($\delta^{13}C_{x-1}$) and ($\delta^{13}C_{x,inlet}$) are the respective isotopic compositions.

311 **2.6.4. Estimation of uncertainties**

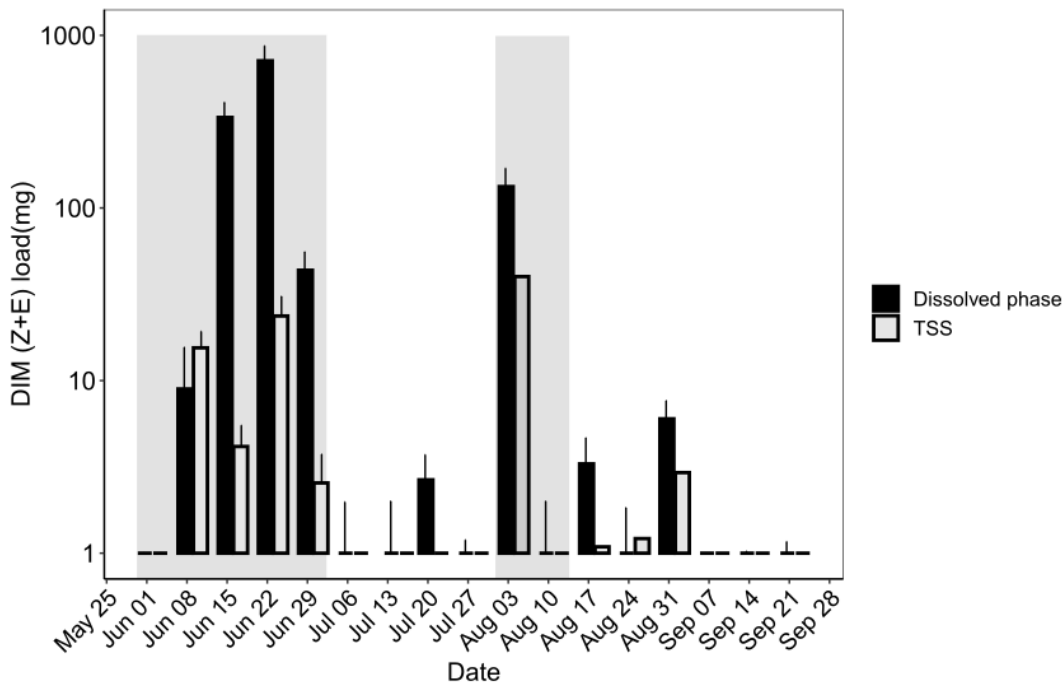
312 The uncertainties associated with pesticide loads (Equation 4) and degradation estimates
 313 (Equations 2, 5, and 6) were calculated via error propagation by accounting for errors associated
 314 with (i) the terms of the hydrological mass balance (Section 2.6.1), including the water depth
 315 measurement in the inlet venturi channel (range ± 2 mm compared to the recorded water depth),
 316 (ii) the topographical/elevation data for the forebay, stone barrier, and sediment zone water volume
 317 (range: ± 5 cm), and (iii) the total analytical errors associated with DIM quantification and CSIA.

318

319 **3. Results and discussion**

320 **3.1. Hydrological dynamics and DIM load entering the wetland**

321 From June 2nd to September 28th, 1059 m³ of surface runoff from the upstream vineyard
322 catchment entered the wetland, while direct rainfall on the wetland contributed 83 m³. Outflow and
323 evapotranspiration reached 928 m³ and 254 m³, respectively. The simulated water volume in the
324 wetland varied from 9 to 184 m³. The sampling campaign was divided into two periods based on
325 hydrological dynamics. Two periods from June 30th to August 1st and from August 11th to
326 September 28 were defined as "dry" as entering runoff or stored volume did not generate outflow.
327 During the dry periods, the wetland was considered a half-closed system, i.e., without outflow and
328 with evapotranspiration only. In contrast, during the wet periods with outflow, the wetland behaved
329 as an open system.



330 **Figure 1.** Load of DIM (Z+E) in dissolved and total suspended solids (TSS) phases of runoff
331 entering the stormwater wetland (Rouffach, France). The shaded area corresponds to wet periods

332 with outflow. The error bars associated with the DIM loads correspond to the propagated error
333 (Section 2.6.4)

334 The DIM loads (Equation 4) from the upstream catchment and entering into the wetland
335 were 100 times higher during wet than during dry periods, with the highest occurrence and loads
336 of DIM observed in the dissolved phase (Figure 1). Other pesticides detected during the study are
337 presented in Section S6. Strong storm events mobilized significant amounts of TSS and associated
338 DIM from the vineyard plots. For instance, a single intense storm event on August 2nd (peak flow
339 velocity at inlet: 91 L/s) mobilized a DIM load associated with TSS (46 ± 9 mg) that was equivalent
340 to the total DIM load in June (40 ± 7 mg) (Figure 1). The loads of DIM Z in the dissolved phase
341 (952 ± 175 mg) and total suspended solids (TSS) (200 ± 29 mg) were three times higher than loads
342 of DIM E (Table S4).

343 The concentrations of DIM found in the runoff samples varied from below the detectable
344 limit (1 ng/L) up to 2.2 μ g/L in the dissolved phase. Based on the toxic unit (TU) (Inostroza et al.,
345 2018) and a toxicity database (Olker et al., 2022), these concentrations may cause adverse chronic
346 effects in fish (TU>1) but not in algae (TU<1). This underscores the importance of intercepting
347 DIM surface runoff from the vineyard catchment to prevent downstream impacts.

348 **3.2. DIM degradation assays**

349 DIM degradation assays were conducted to evaluate DIM degradation in the wetland
350 compartments and to retrieve isotope fractionation values to establish the isotope mass balance
351 using CSIA data. The assays emphasized significantly different kinetics and isotope fractionation
352 values for DIM photodegradation in water and DIM degradation in oxic water with and without
353 plants (Common duckweed) and in anoxic sediments (Table 1).

354 **Table 1.** Results of DIM E and Z laboratory degradation assays. The duration of laboratory
 355 assays varied among the experiments and conditions. n.s. means within the uncertainty range.

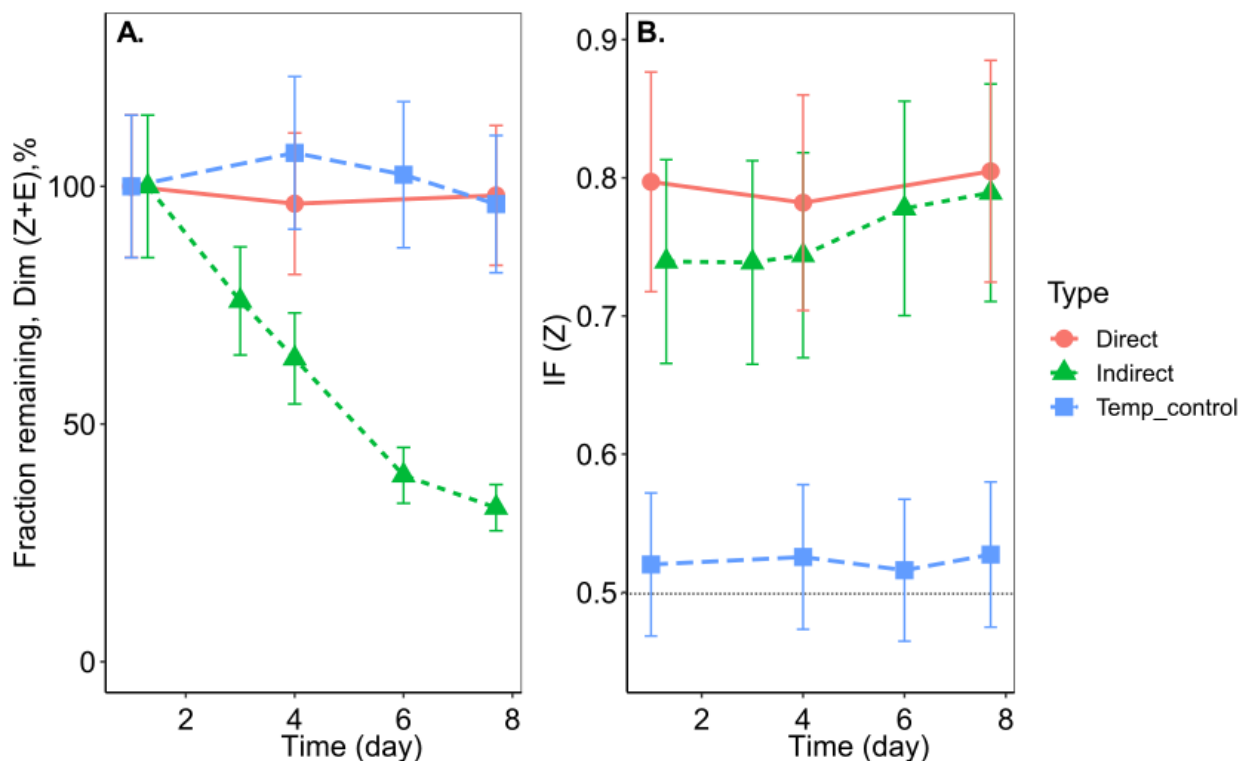
Experiment	Condition	Degradation (%)	Isotope fractionation (ϵ) (‰)	Inversion between isomers	Half-life ($t_{1/2}$) (d)
Photodegradation (indirect)	oxic	75 (sum E+Z)	n.s.	E isomer into Z	15.3 ± 2.2 for sum E+Z
Biodegradation, water	oxic	n.s.	n.s.	n.s.	-
Biodegradation, water, and plant	oxic	45 (E), 30 (Z)	n.s.	n.s.	56-62 (E) and 82-103 (Z)
Biodegradation sediment	anoxic	96 (E) and 96 (Z)	-3.0 ± 0.6 (E) -2.0 ± 0.2 (Z)	n.s.	1.2 ± 0.6 (E) and 1.5 ± 0.8 (Z)

356

357 3.2.1. DIM direct and indirect photodegradation

358 DIM underwent rapid (<24 h) inversion from the E to Z isomer (IF(Z) – 0.8) in indirect
 359 photodegradation experiments with synthetic wetland water and in direct photodegradation
 360 experiments (Figure 2) as already observed previously (Avetta et al., 2014). In contrast, IF(Z)
 361 concentration did not vary significantly in the dark control experiment, confirming that light
 362 exposure caused the inversion from the E to Z isomer of DIM. Up to 75% DIM (Z+E) was degraded
 363 within 8 days under laboratory conditions, corresponding to a half-life of 15.3 ± 2.2 days under
 364 field conditions, i.e., 5.21 peak sun hours per day.

365 No carbon isotope fractionation was observed for both isomers during photodegradation
366 (Figure S5) since radical formation likely occurred irrespective of the presence of heavy and light
367 isotopes (Rosario-Ortiz and Canonica, 2016). The reaction may proceed by radical addition to the
368 double bond of DIM, resulting in the formation of an alkyl radical. Since the radical may be formed
369 at the (R1R2C=) carbon or the (=CH(CO) carbon, the reaction would mainly produce 4-
370 chlorophenyl-3,4-dimethoxyphenyl methanone (CPMPM) or N-formyl morpholine, respectively
371 (Al Rashidi et al., 2013; Avetta et al., 2014). CPMPM was detected in photodegradation experiment
372 samples but only in trace amounts (data not shown). Similar to anoxic biodegradation (Section
373 3.2.3), a mono-demethylated transformation product was also detected, but in small quantities
374 (<3% of the initial DIM amount). Therefore, the DIM transformation pathway during
375 photodegradation could not be elucidated, likely due to the further degradation of unknown DIM
376 transformation products.



377
 378 **Figure 2.** Fraction remaining (%) of DIM (Z and E isomers) (A) and isomeric ratio IF(Z) of DIM
 379 (B) during direct and indirect photodegradation experiments and in dark control experiments. The
 380 dotted black line in panel B represents the IF(Z) ratio of a standard.

381 3.2.2. DIM degradation in wetland water with and without plants

382 In the oxic biodegradation experiments, DIM Z and DIM E did not degrade for 120 days in
 383 the wetland water without duckweed (Figure S6). However, DIM Z and DIM E showed moderate
 384 degradation in experiments with duckweeds in both autoclaved and nonautoclaved wetland water
 385 (Figure S7A). In contrast, DIM was not significantly ($p \geq 0.36$) degraded in the corresponding
 386 control experiments (Figure S7B), indicating that moderate and slow DIM degradation was
 387 associated with the presence of duckweeds.

388 The degradation of DIM in experiments involving duckweeds was driven either by the plant
389 itself or its associated microbiome. To accurately assess DIM mass in the microcosm, the
390 calculations accounted for DIM concentrations in the plant to include DIM plant uptake and
391 sorption. The half-lives of DIM Z (from 82 and 103 days) were longer than those of DIM E (from
392 56 and 62 days) in both experiments with wetland water and plants and with autoclaved wetland
393 water and plants (Table 1). This suggests the preferential degradation of DIM E, although shorter
394 half-lives (from 2.1 to 3.7 days in potato plants) for DIM degradation in plants have been previously
395 reported (Chen et al., 2018; Yang et al., 2022). However, DIM analysis indicated no carbon stable
396 isotope fractionation, either because only a minor (<45%) degradation of DIM was observed after
397 45 days (Figure S8) or due to the absence of isotope fractionation during plant-associated
398 biodegradation. Overall, these results revealed that plant degradation associated with duckweeds
399 may not be a prevailing dissipation process for DIM in stormwater wetlands.

400 **3.2.3. DIM degradation in the wetland sediment**

401 The dissipation half-lives of DIM E and Z in the wetland sediment were 1.2 ± 0.6 and 1.5
402 ± 0.8 days, respectively, which were one and two orders of magnitude higher than in
403 photodegradation and degradation in water with duckweeds, respectively. DIM concentrations did
404 not significantly change in the abiotic controls, excluding significant DIM abiotic degradation.
405 These half-lives are consistent with the reported half-lives of DIM (EFSA, 2006; Masbou et al.,
406 2022), indicating slower degradation of the Z isomer in aerobic and field studies.

407 Stable isotope fractionation observed for both DIM Z and E confirmed the occurrence of *in*
408 *situ* biodegradation in the sediment. The ϵ_C values were $-2.0 \pm 0.2\text{‰}$ and $-3.0 \pm 0.6\text{‰}$ for DIM Z
409 and E, respectively (Figure S9). Variations of ϵ_C between geometric isomers (DIM Z and E) can be

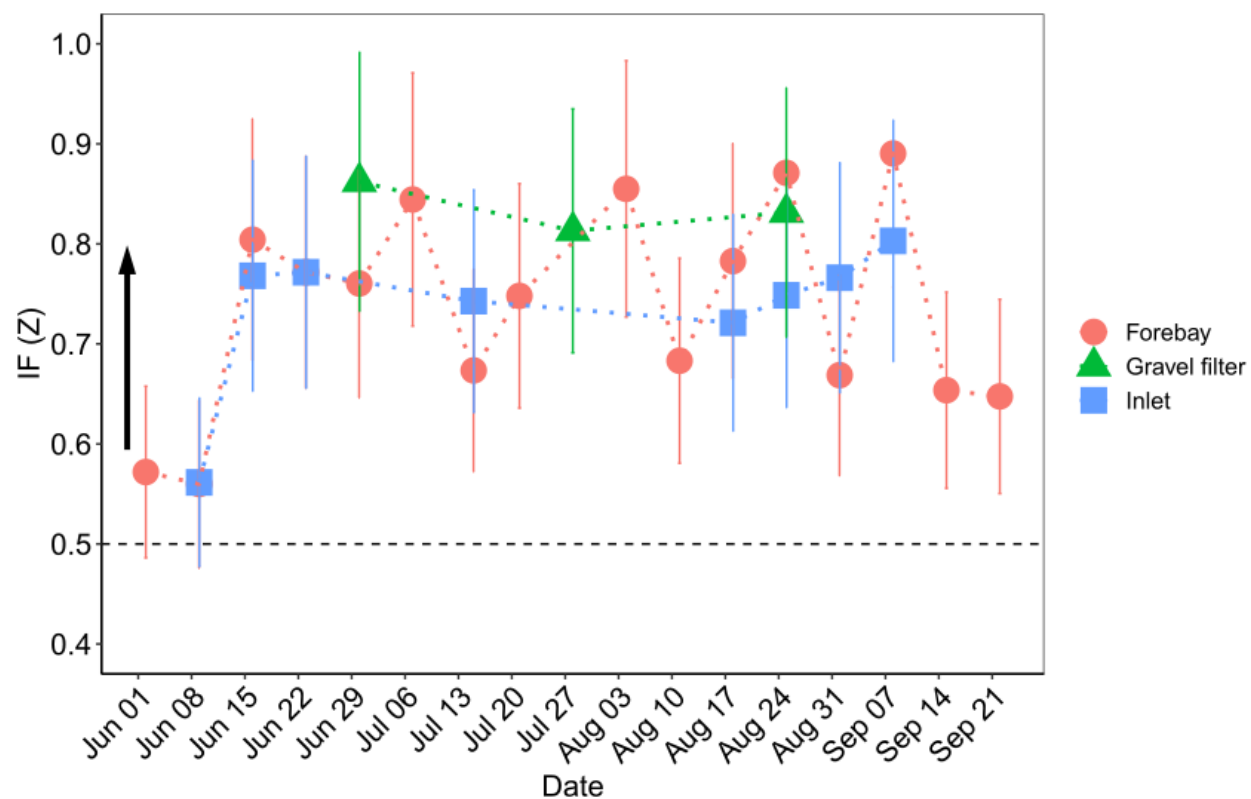
410 attributed to differences in their electronic structures and steric effects, as observed during the
411 anaerobic degradation of compounds like *cis*- and *trans*-1, 2-dichloroethene (Hunkeler et al., 2002).
412 This is the first report of isotope fractionation during DIM degradation under anoxic conditions.
413 Close but lower isotopic fractionation values ($\epsilon_{\text{DIM-(Z)}} = -1.6 \pm 0.2\text{‰}$ and $\epsilon_{\text{DIM-(E)}} = -1.5 \pm 0.2\text{‰}$)
414 were recently reported for degradation in oxic vineyard soils (Masbou et al., 2023). Under oxic
415 conditions, DIM degradation by the strain *Bacillus cereus WL08* has been proposed to start with
416 the oxidative cleavage of the carbon double bond (Zhang et al., 2020). Under anoxic conditions,
417 DIM degradation to mono-demethylated products (EFSA, 2006) which, have also been detected in
418 wetland sediments (data not shown), was reported. Although microorganisms capable of degrading
419 DIM under anoxic conditions are not known and were not examined in this study, it is worth noting
420 that different bacteria associated with the Firmicutes phylum, which were abundant in the
421 sediments (Figure S10), have been shown to possess the ability to O-demethylate organic
422 compounds (Levy-Booth et al., 2021). DIM degradation to mono-demethylated products would
423 imply C-O bond cleavage, with a maximum value of the kinetic isotope effect of ~ 1.061 based on
424 the semiclassical Streitwieser limit (Elsner, 2010). This is consistent with the apparent kinetic
425 isotope effect (AKIE) values for C-O oxygen bond cleavage for isomer Z (1.044 ± 0.004) and
426 isomer E (1.064 ± 0.012) (SI, Section S5).

427 **3.3. Isomer fractionation of DIM in the stormwater wetland**

428 The degradation experiments demonstrated that the degradation potential of DIM isomers
429 largely varied among wetland compartments. Moreover, DIM E degrades faster than DIM Z,
430 although sunlight exposure converts it quickly into DIM Z. Hence, the IF(Z) (isomeric ratio) was
431 used to examine DIM transformation in the stormwater wetland.

432 At the beginning of the study (June 2nd), the IF(Z) ratio of DIM entering in the wetland was
433 close to 0.5 (Figure 3), corresponding to the isomeric ratio of DIM in the commercial formulations
434 (GRIP TOP®) applied in the vineyard between the end of May to the end of June (Masbou et al.,
435 2022). From the 16th of June onwards, the IF(Z) of DIM in runoff entering the wetland gradually
436 increased to 0.83 (IF(Z)>0.5 featuring enrichment in DIM Z). Such an increase in IF(Z) over time
437 was also observed in the vineyard soil and the runoff water, which may reflect DIM biodegradation
438 in soil and/or via light exposure (Masbou et al., 2022).

439 The IF(Z) in the wetland forebay reached 0.8 on the 16th of June and then fluctuated from
440 0.65 to 0.90 throughout the study period (Figure 3). Several co-occurring processes, including
441 biodegradation, photodegradation, mixing, and desorption from sediments, may have affected the
442 DIM isomeric ratios in the wetland. However, vegetation fully covered the wetland by the end of
443 July, which likely limited the effect of light on isomerization. This, along with the rapid degradation
444 of DIM in the wetland sediment, supports the idea that higher IF(Z) ratios in the water of the
445 forebay and the gravel filter indicate DIM biodegradation in the wetland sediment. The subsequent
446 section extends the analysis from isomeric ratios to the exploration of the isotopic ratios of DIM Z
447 in the wetland.



448

449 **Figure 3.** Isomer fraction IF(Z) of DIM in the water of the inlet (blue squares), forebay (red circles),
 450 and gravel filter (green triangles) area of the stormwater wetland (Rouffach, France). The dashed
 451 line represents the IF(Z) of the applied formulation. An arrow indicates preferential E degradation
 452 from June onwards. The error associated with IF(Z) represents the analytical uncertainties of
 453 isomer measurements (n >3).

454 **3.4. Carbon stable isotope fractionation of DIM Z in the stormwater wetland**

455 The DIM Z isotope signatures ($\delta^{13}\text{C}$) in the wetland grab water samples were measured
 456 with a high preconcentration factor ($\times 20,000$ -fold) down to DIM Z concentrations of 88 ng/L. The
 457 POCIS were also used to measure DIM Z $\delta^{13}\text{C}$ after 30 days of deployment in the wetland forebay.
 458 While POCIS measurements represent an integrative $\delta^{13}\text{C}$ value over 30 days, punctual $\delta^{13}\text{C}$ values
 459 were retrieved from the grab water samples from the wetland (Gilevska et al., 2022a).

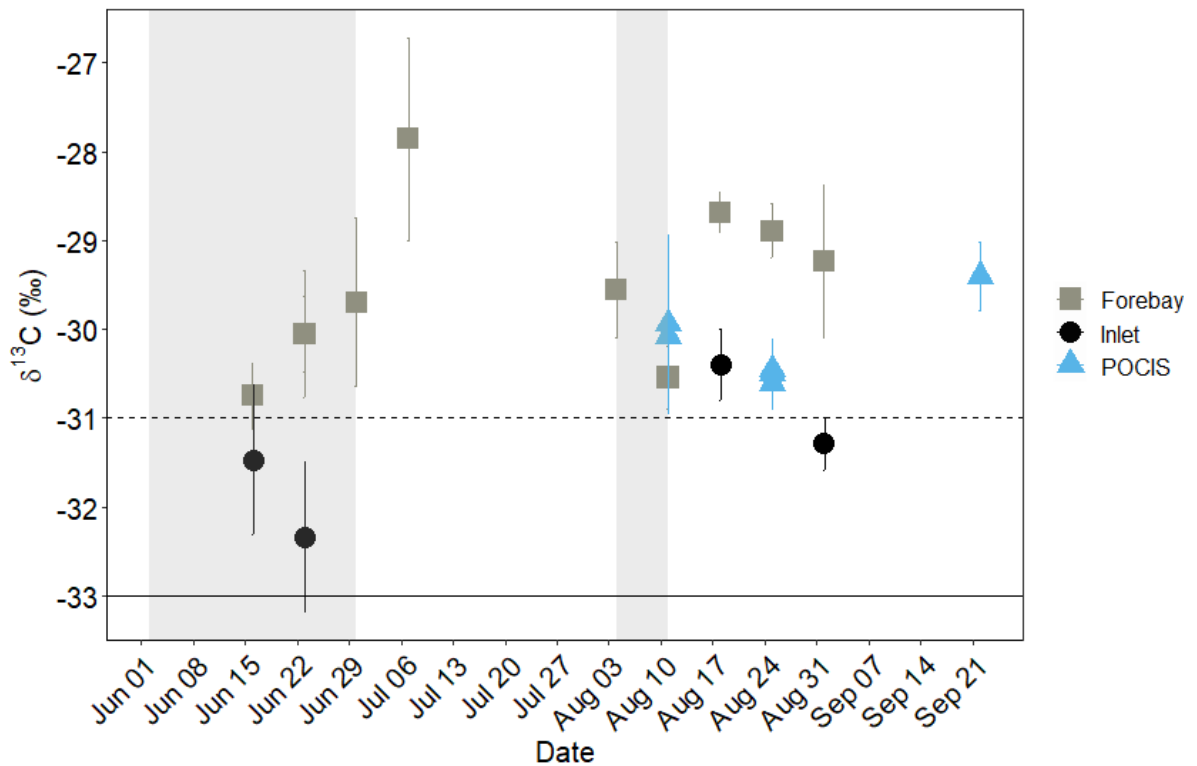
460 The source signature in this study was the stable isotope composition ($\delta^{13}\text{C}$) of the
461 commercially applied formulation in the Rouffach catchment (GRIP TOP®; $\delta^{13}\text{C} = -33.0 \pm 0.3\text{‰}$),
462 which was compared to the $\delta^{13}\text{C}$ values from the POCIS and grab water samples. The changes in
463 the $\delta^{13}\text{C}$ of DIM Z in the wetland were attributed to DIM biodegradation in the sediment (Table 1).
464 Indeed, photo- and plant-associated degradation did not cause significant isotope fractionation in
465 laboratory experiments, while abiotic degradation in control microcosms was insignificant. A
466 threshold of $\Delta(^{13}\text{C}) > 2\text{‰}$ was used to determine significant carbon isotope fractionation caused by
467 DIM transformation (Figure 6) (Hunkeler et al., 2008). A significant isotope fractionation
468 ($\Delta(^{13}\text{C}) > 2\text{‰}$) corresponded to more than 60% DIM Z anaerobic sediment degradation, accounting
469 for the error in the fractionation factor value (Equation 1).

470 The similarity of $\delta^{13}\text{C}$ values of DIM Z in the runoff water entering the wetland and GRIP
471 TOP® formulation (Figure 4), except on August 18th, suggested that the extent of DIM Z
472 degradation in the vineyard soil was generally too small to be detected using CSIA. While DIM
473 degradation in the soil may prevail in specific areas, it is likely that the cumulative runoff primarily
474 consists of undegraded DIM exported from vineyard plots. These findings differ from those of
475 (Masbou et al., 2022), who reported significant degradation of DIM Z in the vineyard soil of the
476 upstream catchment in 2016 and 2017. This difference could be explained by the interannual
477 variability in environmental conditions affecting DIM degradation in soil, such as rainfall,
478 temperature, soil properties, and agricultural practices.

479 Overall, the grab samples provided punctual information on *in situ* degradation in the
480 wetland whereas POCIS samples were affected by fresh inputs of undegraded DIM in the runoff
481 entering the wetland (Figure 4). The grab samples were more able to capture DIM Z isotopic
482 signatures in the wetland, with $\delta^{13}\text{C}$ values of DIM Z showing significant enrichment in ^{13}C ($2.0 \geq$

483 $\delta^{13}\text{C} \leq 5.1\text{‰}$) compared to those of GRIP TOP[®]. The difference in the $\delta^{13}\text{C}$ values between the inlet
484 and forebay samples ($\Delta(^{13}\text{C})$ of 3.0‰, Figure 4) over time also confirmed the *in situ* biodegradation
485 of DIM Z.

486 Based on laboratory experiments, it was expected that rapid DIM biodegradation mainly
487 occurred in the wetland sediment. Microorganisms associated with DIM biodegradation were likely
488 more abundant in sediments than in the water column, explaining the very low concentrations of
489 DIM in the sediments, which limited DIM CSIA. In contrast, light penetration (first 10 cm of water
490 column) in natural waters (Mathon et al., 2019) is generally limited, and DIM photodegradation
491 only contributed to DIM degradation in June, when the wetland was not covered by duckweeds
492 (Figure S2).



493

494 **Figure 4.** $\delta^{13}\text{C}$ values of DIM Z from grab water samples at the inlet (black circle), and forebay
495 (grey squares) areas of the stormwater wetland (Rouffach, France) and from POCIS (blue triangle).
496 The dashed line represents the 2‰ range from the carbon isotope value of the pure product (GRIP
497 TOP®, -33.0‰) represented by the solid line. The shaded area corresponds to wet periods, with
498 water outflow from the wetland. The error bar represents the reproducibility of the measurements
499 ($n \geq 3$).

500 **3.5. Quantitative estimates of DIM Z biodegradation in the wetland**

501 A concentration-based mass balance was used to quantify the extent of dissipation and
502 degradation of all detected pesticides in the stormwater wetland (SI, Section S7). Mass balances
503 based on DIM Z concentrations (Equation 5) and stable isotope data (Equation 2 and 6) provided
504 similar estimates for the extent of DIM Z degradation and indicated significant ($>46 \pm 20\%$) DIM
505 Z degradation over the study period (Table 2). Interestingly, the extent of DIM Z degradation
506 during the two dry periods was similar, despite their different durations (Table 2). The agreement
507 between both mass balance approaches is remarkable considering their different conceptual and
508 methodological basis. This confirms the validity of using CSIA for evaluating the contribution of
509 pesticide degradation in wetland systems.

510

511

512

513 **Table 2.** Degradation estimates of DIM Z in the stormwater wetland (Rouffach, France) for the
 514 wet and dry periods using the classical (Equation 5) and isotope mass balance approaches
 515 (Equations 2 and 6). n.a.: not applicable due to a lack of outflow monitoring.

Period	Degradation extent (%)	
	Classical mass balance	Isotope mass balance
Wet period (June 2 nd - June 30 th)	n.a.	71 ± 18
Dry period (June 30 th – August 1 st)	94 ± 22	61 ± 26
Wet period (August 1 st – August 11 th)	n.a.	46 ± 20
Dry period (August 11 th – September 22 nd)	86 ± 18	68 ± 17

516

517 In the classical mass balance approach, the accuracy of pesticide degradation estimates
 518 largely depends on the physicochemical properties of the compound and the consideration of
 519 processes and compartments assumed to be involved in pesticide degradation. For instance, DIM
 520 degradation could be estimated with this approach, since DIM is not volatile (Lewis et al., 2006)
 521 and its sorption or uptake in plants and sediments was accounted for in our study. However,
 522 extensive field and laboratory work is required to account for all processes and compartments
 523 potentially involved in pesticide degradation and their dynamics.

524 It is also noteworthy that degradation based on concentration mass balance was estimated
 525 by assuming that the pesticide detection limits were similar across wetland compartments.
 526 However, the detection limits for pesticides in the dissolved phase were >1000-fold lower than
 527 those in the sediment, plant, or TSS samples since large (up to 12 L) water volumes were processed
 528 (Gilevska et al., 2022b). Such differences in detection limits among wetland compartments can
 529 lead to a severe overestimation of pesticide dissipation, which may explain the higher estimates of

530 DIM Z degradation in the stormwater wetland using the classical mass balance approach. In
531 addition, the estimation of pesticide concentrations in the TSS from the wetland runoff may be
532 inaccurate due to the variability in the TSS concentration (32 to 378 mg/L) in runoff entering the
533 wetland. This variability can lead to the collection of small and poorly representative amounts of
534 TSS during periods of low or moderate runoff, which can further bias the actual pesticide loads
535 measured in the TSS.

536 In this context, the main advantage of estimating pesticide biodegradation using CSIA is
537 that it relates changes in the isotopic composition of the target pesticide to its degradation, which
538 is typically not influenced by nondegradative processes, such as sorption or volatilization
539 (Hunkeler et al., 2008). This may result in more accurate and reliable estimates of biodegradation.
540 However, systematic and lab-intensive reference degradation experiments are required to retrieve
541 isotope fractionation values, if they do not already exist, and to identify transformation pathways.
542 In the case of DIM Z, carbon stable isotope analysis (CSIA) primarily indicated biodegradation in
543 the wetland sediment, with no observed isotopic fractionation during DIM photodegradation. This
544 suggests that relying solely on isotope data for estimating DIM Z degradation in wetlands may
545 underestimate its extent if non-fractionating degradative processes play a significant role, thus
546 rendering such degradation estimates conservative. When the estimation of DIM Z degradation
547 extent is extended to both isomers of DIM using the isotope approach, it reinforces a more cautious
548 perspective. This is because laboratory experiments have shown that DIM E, the second isomer, is
549 more degradable compared to DIM Z.

550 The isotope mass balance approach was also advantageous in estimating DIM Z degradation
551 during wet periods (Table 2). In fact, isotope fractionation can be directly related to degradation,
552 and thus, a closed hydrological mass balance with inlet and outlet sampling is not needed. Notably,

553 DIM Z degradation during the second wet period was lower than that during the first wet period. It
554 can be hypothesized that the high input loads of DIM Z into the wetland during the intense storm
555 event on August 2nd reduced the DIM Z residence and reaction time in the wetland and thus the
556 extent of biodegradation ($46 \pm 20\%$, Table 2). Hence, pesticide dissipation, including
557 biodegradation, in stormwater wetlands receiving runoff from agricultural catchments may largely
558 vary depending on the runoff regime.

559 **3. Conclusion**

560 The contribution of pesticide degradation in wetlands intercepting agricultural runoff is often
561 overlooked and confounded with other dissipation processes when quantified based on pesticide
562 concentrations alone. This study confirms the potential of wetland systems for pesticide dissipation
563 and the crucial role of wetland sediments in pesticide degradation. It also highlights the variability
564 of pesticide removal in stormwater wetlands, depending on hydro-climatic dynamic. The CSIA
565 approach enabled to evaluate DIM Z degradation in a stormwater wetland, showing its
566 complementarity with traditional concentration-based methods. Estimates of DIM Z degradation
567 using concentration and CSIA data in the stormwater wetland were similar, which validated the
568 CSIA approach. The laboratory degradation assays identified wetland sediments as the primary
569 compartment controlling DIM degradation, emphasizing the need to evaluate co-occurring
570 processes to understand pesticide dissipation in wetland systems. Additionally, the DIM isomer
571 ratio (Z and E) was a sensitive proxy for the occurrence and intensity of DIM degradation.
572 Altogether, this study highlights the relevance of combining multiple lines of evidence, including
573 field surveys and laboratory experiments, and using concentration-, isotope- and isomer-based
574 approaches, to evaluate and quantify pesticide transformation in wetland systems. Future research
575 may benefit from monitoring transformation products during pesticide degradation to distinguish

576 incomplete and complete mineralization, and from multi-element CSIA to offer further insights
577 into pesticide degradation pathways in wetlands.

578 **Author contribution statement**

579 **Tetyana Gilevska:** Conceptualization, Investigation, Writing - Original Draft. **Sylvain**
580 **Payraudeau:** Conceptualization, Data Curation, Writing - Review & Editing. **Gwenaël Imfeld:**
581 Conceptualization, Writing - Review & Editing, Project Management, Funding acquisition.

582 **Declaration of competing interest**

583 The authors declare that they have no known competing financial interests or personal
584 relationships that could have appeared to influence the work reported in this paper.

585 **Acknowledgment**

586 The study and the fellowship of Tetyana Gilevska were funded by the French National Research
587 Agency ANR through grant ANR-18-CE32-0007, project PESTIPOND. The authors thank the City
588 of Rouffach for holding the stormwater wetland. The authors wish to acknowledge Tobias
589 Junginger, Benoit Guyot, Eric Pernin, and Thierry Perrone for support in sampling and surveys,
590 Jeremy Masbou for assistance in screening transformation products and useful discussion, and
591 Marina Debret for her contribution to topographic surveying with theodolite and data processing.

592

593

594 **References**

595 Al Rashidi, M.J., Chakir, A. and Roth, E. 2013. Heterogeneous Ozonolysis of Folpet and Dimethomorph:
596 A Kinetic and Mechanistic Study. J Phys Chem A 117(14), 2908-2915.

597 Alvarez-Zaldivar, P., Payraudeau, S., Meite, F., Masbou, J. and Imfeld, G. 2018. Pesticide degradation and
598 export losses at the catchment scale: Insights from compound-specific isotope analysis (CSIA).
599 *Water Res* 139, 198-207.

600 Avetta, P., Marchetti, G., Minella, M., Pazzi, M., De Laurentiis, E., Maurino, V., Minero, C. and Vione, D.
601 2014. Phototransformation pathways of the fungicide dimethomorph ((E,Z) 4-[3-(4-chlorophenyl)-
602 3-(3,4-dimethoxyphenyl)-1-oxo-2-propenyl]morpholine), relevant to sunlit surface waters. *Sci*
603 *Total Environ* 500-501, 351-360.

604 Barillot, C.D., Sarde, C.-O., Bert, V., Tarnaud, E. and Cochet, N. 2013. A standardized method for the
605 sampling of rhizosphere and rhizoplan soil bacteria associated to a herbaceous root system. *Annals*
606 *of microbiology* 63(2), 471-476.

607 Chen, C., Luo, J.H., Zhang, W.W., Bu, C.C. and Ma, L.M. 2022. Pesticide degradation in an integrated
608 constructed wetland: Insights from compound-specific isotope analysis and 16S rDNA sequencing.
609 *Sci Total Environ* 841.

610 Chen, L., Jia, C.H., Li, F.G., Jing, J.J., Yu, P.Z., He, M. and Zhao, E.C. 2018. Dissipation and residues of
611 fluazinam and dimethomorph in potatoes, potato plants, and soil, determined by QuEChERS ultra-
612 performance liquid chromatography tandem mass spectrometry. *Environ Sci Pollut R* 25(32),
613 32783-32790.

614 Coplen, T.B. 2011. Guidelines and recommended terms for expression of stable-isotope-ratio and gas-ratio
615 measurement results. *Rapid Commun Mass Sp* 25(17), 2538-2560.

616 Duplay, J., Semhi, K., Errais, E., Imfeld, G., Babcsanyi, I. and Perrone, T. 2014. Copper, zinc, lead and
617 cadmium bioavailability and retention in vineyard soils (Rouffach, France): The impact of cultural
618 practices. *Geoderma* 230, 318-328.

619 EFSA 2006. Conclusion on the peer review of the pesticide risk assessment of the active substance
620 dimethomorph. *EFSA Scientific Report* (2006) 82, 1-69.

621 Elsayed, O.F., Maillard, E., Vuilleumier, S., Nijenhuis, I., Richnow, H.H. and Imfeld, G. 2014. Using
622 compound-specific isotope analysis to assess the degradation of chloroacetanilide herbicides in lab-
623 scale wetlands. *Chemosphere* 99, 89-95.

624 Gilevska, T., Masbou, J., Baumlin, B., Chaumet, B., Chaumont, C., Payraudeau, S., Tournebize, J., Probst,
625 A., Probst, J.L. and Imfeld, G. 2022a. Do pesticides degrade in surface water receiving runoff from
626 agricultural catchments? Combining passive samplers (POCIS) and compound-specific isotope
627 analysis. *Sci Total Environ* 842, 156735.

628 Gilevska, T., Wiegert, C., Droz, B., Junginger, T., Prieto-Espinoza, M., Borreca, A. and Imfeld, G. 2022b.
629 Simple extraction methods for pesticide compound-specific isotope analysis from environmental
630 samples. *MethodsX*, 101880.

631 Grégoire, C., Elsaesser, D., Huguenot, D., Lange, J., Lebeau, T., Merli, A., Mose, R., Passeport, E.,
632 Payraudeau, S. and Schütz, T. 2009. Mitigation of agricultural nonpoint-source pesticide pollution
633 in artificial wetland ecosystems—a review. *Climate Change, Intercropping, Pest Control and*
634 *Beneficial Microorganisms*, 293-338.

635 Grégoire, C., Payraudeau, S. and Domange, N. 2010. Use and fate of 17 pesticides applied on a vineyard
636 catchment. *International Journal of Environmental and Analytical Chemistry* 90(3-6), 406-420.

637 Honsberg, C. and Bowden, S.G. 2019. Photovoltaics education website. PV Education.

638 Hunkeler, D., Aravena, R. and Cox, E. 2002. Carbon isotopes as a tool to evaluate the origin and fate of
639 vinyl chloride: Laboratory experiments and modeling of isotope evolution. *Environ Sci Technol*
640 36(15), 3378-3384.

641 Hunkeler, D., Meckenstock, R.U., Sherwood Lollar, B., Schmidt, T.C., Wilson, J.T., Schmidt, T. and
642 Wilson, J. 2008. A guide for assessing biodegradation and source identification of organic ground
643 water contaminants using compound specific isotope analysis (CSIA). US EPA, Ada.

644 Imfeld, G., Meite, F., Wiegert, C., Guyot, B., Masbou, J. and Payraudeau, S. 2020. Do rainfall
645 characteristics affect the export of copper, zinc and synthetic pesticides in surface runoff from
646 headwater catchments? *Sci Total Environ* 741, 140437.

647 Imfeld, G., Payraudeau, S., Tournebize, J., Sauvage, S., Macary, F., Chaumont, C., Probst, A., Sánchez-
648 Pérez, J.-M., Bahi, A. and Chaumet, B. 2021. The role of ponds in pesticide dissipation at the
649 agricultural catchment scale: A critical review. *Water* 13(9), 1202.

650 Inostroza, P.A., Vera-Escalona, I., Wild, R., Norf, H. and Brauns, M. 2018. Tandem Action of Natural and
651 Chemical Stressors in Stream Ecosystems: Insights from a Population Genetic Perspective. *Environ*
652 *Sci Technol* 52(14), 7962-7971.

653 Koli, P., Bhardwaj, N.R. and Mahawer, S.K. (2019) *Climate change and agricultural ecosystems*, pp. 65-
654 94, Elsevier.

655 Levy-Booth, D.J., Hashimi, A., Roccor, R., Liu, L.Y., Renneckar, S., Eltis, L.D. and Mohn, W.W. 2021.
656 Genomics and metatranscriptomics of biogeochemical cycling and degradation of lignin-derived
657 aromatic compounds in thermal swamp sediment. *ISME J* 15(3), 879-893.

658 Lewis, K., Tzilivakis, J., Green, A. and Warner, D. 2006. Pesticide Properties DataBase (PPDB).

659 Lissalde, S., Mazzella, N., Fauvelle, V., Delmas, F., Mazellier, P. and Legube, B. 2011. Liquid
660 chromatography coupled with tandem mass spectrometry method for thirty-three pesticides in
661 natural water and comparison of performance between classical solid phase extraction and passive
662 sampling approaches. *J Chromatogr A* 1218(11), 1492-1502.

663 Lucas, Y., Schmitt, A., Chabaux, F., Clément, A., Fritz, B., Elsass, P. and Durand, S. 2010. Geochemical
664 tracing and hydrogeochemical modelling of water–rock interactions during salinization of alluvial
665 groundwater (Upper Rhine Valley, France). *Applied Geochemistry* 25(11), 1644-1663.

666 Maillard, E. and Imfeld, G. 2014. Pesticide mass budget in a stormwater wetland. *Environ Sci Technol*
667 48(15), 8603-8611.

668 Maillard, E., Payraudeau, S., Faivre, E., Gregoire, C., Gangloff, S. and Imfeld, G. 2011. Removal of
669 pesticide mixtures in a stormwater wetland collecting runoff from a vineyard catchment. *Sci Total*
670 *Environ* 409(11), 2317-2324.

671 Masbou, J., Drouin, G., Payraudeau, S. and Imfeld, G. 2018. Carbon and nitrogen stable isotope
672 fractionation during abiotic hydrolysis of pesticides. *Chemosphere* 213, 368-376.

673 Masbou, J., Payraudeau, S., Guyot, B. and Imfeld, G. 2022. Dimethomorph degradation in vineyards
674 examined by isomeric and isotopic fractionation. *Chemosphere* 313, 137341.

675 Mathon, B., Coquery, M., Miege, C., Vanduycke, A. and Choubert, J.M. 2019. Influence of water depth and
676 season on the photodegradation of micropollutants in a free-water surface constructed wetland
677 receiving treated wastewater. *Chemosphere* 235, 260-270.

678 Rosario-Ortiz, F.L. and Canonica, S. 2016. Probe Compounds to Assess the Photochemical Activity of
679 Dissolved Organic Matter. *Environ Sci Technol* 50(23), 12532-12547.

680 Schreglmann, K., Hoeche, M., Steinbeiss, S., Reinnicke, S. and Elsner, M. 2013. Carbon and nitrogen
681 isotope analysis of atrazine and desethylatrazine at sub-microgram per liter concentrations in
682 groundwater. *Anal Bioanal Chem* 405(9), 2857-2867.

683 Scott, K.M., Lu, X., Cavanaugh, C.M. and Liu, J.S. 2004. Optimal methods for estimating kinetic isotope
684 effects from different forms of the Rayleigh distillation equation. *Geochimica Et Cosmochimica*
685 *Acta* 68(3), 433-442.

686 Suchana, S., Wu, L. and Passeport, E. 2022. Compound specific carbon, hydrogen, and nitrogen isotope
687 analysis of nitro- and amino-substituted chlorobenzenes using solid phase extraction.

688 Tang, F.H.M., Lenzen, M., McBratney, A. and Maggi, F. 2021. Risk of pesticide pollution at the global
689 scale. *Nature Geoscience* 14(4), 206-210.

690 Yang, L.P., Zheng, Q., Lin, S.K., Wang, Y.Q., Zhu, Q.Z., Cheng, D.M., Chen, J.J. and Zhang, Z.X. 2022.
691 Dissipation and residue of dimethomorph in potato plants produced and dietary intake risk
692 assessment. *Int J Environ Res Public Health* 19(10), 1332-1344.

693 Zhang, C., Li, J.H., Wu, X.M., Long, Y.H., An, H.M., Pan, X.L., Li, M., Dong, F.S. and Zheng, Y.Q. 2020.
694 Rapid degradation of dimethomorph in polluted water and soil by *Bacillus cereus* WL08
695 immobilized on bamboo charcoal-sodium alginate. *J Hazard Mater* 398.

696